

## Conformal aspect of charge density waves: Theory and experiment

Keiji Nakatsugawa<sup>1,2,\*</sup>, Tatsuhiko N. Ikeda,<sup>3</sup> Takeshi Toshima<sup>4</sup>, and Satoshi Tanda<sup>1,5,\*</sup>

<sup>1</sup>Center of Education and Research for Topological Science and Technology, Hokkaido University, Sapporo 060-8628, Japan

<sup>2</sup>Research Center for Materials Nanoarchitectonics, National Institute for Materials Science, Tsukuba 305-0044, Japan

<sup>3</sup>RIKEN Center for Quantum Computing, Wako, Saitama 351-0198, Japan

<sup>4</sup>Department of General Education, National Institute of Technology, Toyama College, Toyama 939-8630, Japan

<sup>5</sup>Department of Applied Physics, Hokkaido University, Sapporo 060-8628, Japan

 (Received 13 March 2023; revised 24 January 2024; accepted 24 January 2024; published 27 February 2024)

The variety of two-dimensional (2D) discommensurate charge density wave (DC-CDW) phases has been explained by a phenomenological CDW free-energy theory, where the wave vector of different DC-CDW phases corresponds to different local minima of a multivalley free-energy landscapes. Here, we discover that experimental 2D DC-CDW structures in transition-metal dichalcogenides can be understood elegantly by a conformal transformation with complex numbers. Specifically, we represent a 2D CDW wave vector  $\mathbf{Q}$  by a complex number  $Q$  and find that by minimizing the CDW free energy with respect to  $Q$ , different wave vectors  $Q$  and  $Q'$  are connected by a conformal transformation. Consequently,  $\sqrt{n} \times \sqrt{n}$  ( $n = 7, 9, 13$ ) honeycomb and (quasi-)stripe DC-CDWs can be understood using simple conformal groups, which link DC-CDW wave vectors (multivalley landscape) to the incommensurate and commensurate wave vectors.

DOI: [10.1103/PhysRevB.109.L081407](https://doi.org/10.1103/PhysRevB.109.L081407)

**Introduction.** Charge density waves (CDWs) are electronic crystals that are described by so-called macroscopic wave functions such as superconductors, superfluids, fractional quantum Hall liquids, etc. [1–3]. Transition-metal dichalcogenides ( $MX_2$ ) are layered compounds that induce typical two-dimensional (2D) CDW phases with wave vectors  $\mathbf{Q}^{(i)}$  ( $i = 1, 2, 3$ ) satisfying the triple-Q condition  $\mathbf{Q}^{(1)} + \mathbf{Q}^{(2)} + \mathbf{Q}^{(3)} = \mathbf{0}$ . Such CDW phases include the incommensurate (IC) phase, commensurate (C) phase, and CDW phases with discommensurate (DC) domain walls, such as the nearly commensurate (NC), stripe [4], and triclinic (T) phases [5,6]. Moreover, other CDW phases are continually being discovered [7–9].

A phenomenological Ginzburg-Landau theory of CDW phases in  $MX_2$  was introduced by McMillan [10] to explain the IC to C phase transition and 1D stripe discommensuration. However, McMillan heuristically included discommensurations, and hence could not correctly explain known CDW phases [11]. Nakanishi and Shiba extended this free energy theory to explain the appearance of the NC phase in  $1T$ -TaS<sub>2</sub> ( $\sqrt{13} \times \sqrt{13}$  structure) and  $2H$ -TaSe<sub>2</sub> ( $\sqrt{9} \times \sqrt{9}$  structure) using CDW harmonics, where the domain walls and harmonic wave vectors are all obtained from the fundamental wave vectors  $\mathbf{Q}^{(i)}$  [12,13]. In general, the search for CDW free energy local minima is a difficult task. Some of the present authors revisited the Nakanishi-Shiba-McMillan models for monolayer  $1T$ -TaS<sub>2</sub> and  $2H$ -TaSe<sub>2</sub> and discovered the multivalley free-energy landscape, where free energy local minima correspond to different DC-CDW phases with domain walls (NC, stripe, and T phases) [14]. The existence of these CDW

phases in monolayer  $MX_2$  (pure 2D system) is confirmed both experimentally [15] and theoretically [14].

Despite the development of CDW free-energy theory, why such different DC-CDW phases can appear in modern quantum crystals is still an open question. The reason for the appearance of various CDW phases is not simply because there are various magnitudes of nesting vectors  $\mathbf{Q}$ . For nesting vectors that happen to be close to the C condition, there seems to be a law that locks in CDW superlattice to the  $MX_2$  lattice. Within the framework of the Nakanishi-Shiba-McMillan theory, we reveal that this law is given by a conformal transformation between DC wave vectors. Here, a conformal transformation refers to a composition of translation, rotation, dilation, and inversion [16].

In this paper, we discover that experimental 2D DC-CDW structures in  $MX_2$  can be explained by a conformal transformation with complex numbers. Specifically, we represent a 2D CDW wave vector  $\mathbf{Q}$  by a complex number  $Q$  and minimize the phenomenological CDW free energy with respect to  $Q$ , which leads to a multivalley free-energy landscape where different wave vectors  $Q$  and  $Q'$  are connected by a conformal transformation. Consequently, we explain  $\sqrt{n} \times \sqrt{n}$  ( $n = 7, 9, 13$ ) honeycomb and (quasi)stripe DC-CDWs using simple conformal groups, which link DC-CDW wave vectors to the IC and C wave vectors. Consequently,  $\sqrt{n} \times \sqrt{n}$  ( $n = 7, 9, 13$ ) honeycomb and (quasi)stripe DC-CDWs can be explained beautifully by a discrete conformal transformation with Eisenstein integers  $\mathbb{Z}[\omega]$ . The CDW phases such as NC, T, and stripes, which seem to be completely unrelated at first glance, actually have a common relation linking their  $\mathbf{Q}$  to  $\mathbf{Q}_{IC}$  and  $\mathbf{Q}_C$ . Then, we apply our conformal method to explain the origin of an experimental NC phase in TaSe<sub>2</sub> thin-film ( $\sqrt{7} \times \sqrt{7}$  structure).

\*These authors contributed equally to this work.

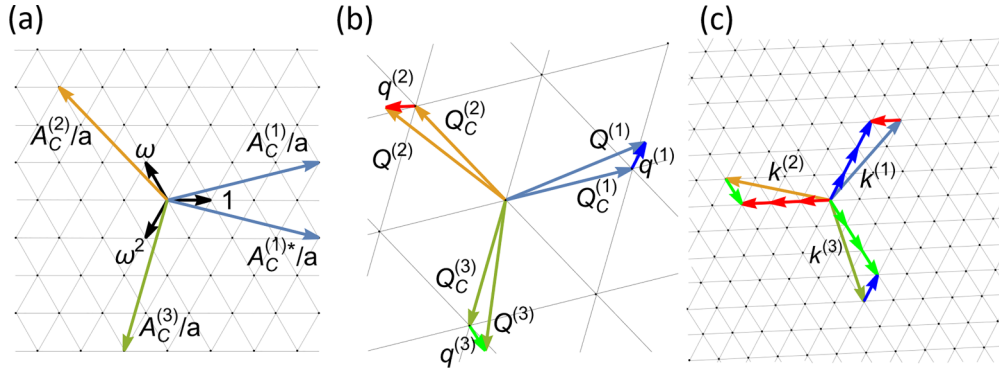


FIG. 1. (a) C-CDW superlattice vectors can be represented by Eisenstein integers (this figure shows the  $\sqrt{13} \times \sqrt{13}$  structure with  $\mu = 3$  and  $\nu = 1$ ). (b) Domain wall wave vectors  $q^{(i)}$  are given as deviation from  $Q_C^{(i)}$ . (c) CDW harmonics  $k^{(i)}$ .

*The commensurate structure and CDW free energy.* First, we review the C structure and CDW free energy theory in  $MX_2$ . Consider a triangular lattice with primitive lattice vectors  $\mathbf{a}_1 = (1, 0)a$  and  $\mathbf{a}_2 = \frac{1}{2}(-1, \sqrt{3})a$  where  $a = \|\mathbf{a}_1\| = \|\mathbf{a}_2\|$ ,  $\|\cdot\|$  represents the norm of a vector. The CDW superlattice vector  $\mathbf{A}_C$  of the C phase is defined as [1]

$$\mathbf{A}_C = (\mu + \nu)\mathbf{a}_1 + \nu\mathbf{a}_2, \quad (1)$$

where  $\mu$  and  $\nu$  are positive integers that depend on materials [e.g.,  $\mu = 3$  and  $\nu = 1$  for the  $\sqrt{13} \times \sqrt{13}$  structure in 1T-TaS<sub>2</sub> as shown in Fig. 1(a)]. Reciprocal lattice vectors  $\mathbf{b}_1$  and  $\mathbf{b}_2$  which satisfy  $\mathbf{a}_i \cdot \mathbf{b}_j = 2\pi\delta_{ij}$  ( $i, j = 1, 2$ ) are given by  $\mathbf{b}_1 = (1, 1/\sqrt{3})/a$  and  $\mathbf{b}_2 = (0, 2/\sqrt{3})/a$ .  $\mathbf{a}_i$  and  $\mathbf{b}_i$  are not parallel but are separated by  $30^\circ$ . However, for the description of CDW it would be convenient to have a set of reciprocal lattice vectors  $\mathbf{G}_i$  which are parallel to  $\mathbf{a}_i$ . From the threefold rotational symmetry of the system, we require that  $\mathbf{G}_1$  and  $\mathbf{G}_2$  are separated by  $120^\circ$  and we also define  $\mathbf{a}_3 = -\mathbf{a}_1 - \mathbf{a}_2$ ,  $\mathbf{G}_3 = -\mathbf{G}_1 - \mathbf{G}_2$ . The two sets of reciprocal lattice vectors are related by  $\mathbf{b}_1 = 2/3(\mathbf{G}_1 - \mathbf{G}_3)$  and  $\mathbf{b}_2 = 2/3(\mathbf{G}_2 - \mathbf{G}_3)$ .  $\mathbf{G}_i$  ( $i = 1, 2, 3$ ) are normalized by the condition  $\mathbf{a}_i \cdot \mathbf{G}_i = 2\pi$ . For  $i \neq j$ ,  $\mathbf{a}_i$  and  $\mathbf{G}_j$  are mutually separated by  $120^\circ$ , which implies  $\mathbf{a}_i \cdot \mathbf{G}_j = 2\pi \cos(2\pi/3) = -\pi$ . Consequently, we have the condition  $\mathbf{a}_i \cdot \mathbf{G}_j = 2\pi\delta_{ij} - \pi(1 - \delta_{ij}) = \pi(3\delta_{ij} - 1)$ . Then, the wave vector which satisfies  $\mathbf{A}_C \cdot \mathbf{Q}_C = 2\pi$  is defined as

$$\mathbf{Q}_C = \frac{(\mu + \nu)\mathbf{G}_1 + \nu\mathbf{G}_2}{\|\mathbf{A}_C\|^2/a^2}, \quad (2)$$

where  $\|\mathbf{A}_C\|/a = \sqrt{\mu^2 + \mu\nu + \nu^2}$ . There are actually three equivalent superlattice vectors  $\mathbf{A}_C^{(1)}$ ,  $\mathbf{A}_C^{(2)}$ ,  $\mathbf{A}_C^{(3)}$ , which are rotated from  $\mathbf{A}_C$  by  $0^\circ$ ,  $120^\circ$ , and  $240^\circ$ , respectively, and three equivalent wave vectors  $\mathbf{Q}_C^{(i)}$ , which are defined likewise (Fig. 1).

We also consider general CDW phases in equilibrium.  $MX_2$  exhibits three types of isotropic CDW phases, where each  $\mathbf{Q}^{(i)}$  is separated by  $120^\circ$ , namely, the IC, NC, and C phases. There are also the anisotropic stripe phase [4,17] and the T phase [5,6].  $\mathbf{Q}_{IC}^{(i)}$  are usually determined by Fermi surface nesting or van Hove singularity [2,3,18–21], which is independent of the underlying lattice. On the other hand,  $\mathbf{Q}_C^{(i)}$  are determined from lattice symmetry and satisfy Eq. (2). DC phases between the C phase and the IC phase have domain

walls (discommensurations) that originate from commensurability with the underlying base lattice [10,12,13,22].

Suppose that  $\mathbf{Q}_{IC}^{(i)}$  and  $\mathbf{Q}_C^{(i)}$  are known. The following free energy, which was originally proposed by McMillan [10], describes the IC-C phase transition

$$F = \int d^2r \left\{ a(\mathbf{r})\alpha(\mathbf{r})^2 - b(\mathbf{r})\alpha(\mathbf{r})^3 + c(\mathbf{r})\alpha(\mathbf{r})^4 + d(\mathbf{r}) \sum_{i=1}^3 |\psi_i(\mathbf{r})\psi_{i+1}(\mathbf{r})|^2 + \sum_{i=1}^3 \psi_i(\mathbf{r})^* e_i(-i\nabla)\psi_i(\mathbf{r}) \right\}. \quad (3)$$

Here,  $\mathbf{r}$  is the 2D spatial coordinate. The complex order parameters  $\psi_i(\mathbf{r})$  are related to the charge density  $\rho(\mathbf{r}) = \rho_0(\mathbf{r})[1 + \alpha(\mathbf{r})]$ , where  $\alpha(\mathbf{r}) = \text{Re}[\psi_1(\mathbf{r}) + \psi_2(\mathbf{r}) + \psi_3(\mathbf{r})]$ .  $\rho_0(\mathbf{r})$  is the charge density in the normal phase. Each coefficient has periodicity of the  $MX_2$  lattice and is written as  $a(\mathbf{r}) = a_0 + 2a_1 \sum_{i=1}^3 \cos(\mathbf{G}_i \cdot \mathbf{r})$ , etc. The third-order term reflects the triple-Q condition  $\mathbf{Q}^{(1)} + \mathbf{Q}^{(2)} + \mathbf{Q}^{(3)} = \mathbf{0}$ . The constant terms  $a_0, b_0, c_0, d_0$  are sufficient to discuss the IC phase, but the Umklapp terms such as  $c_1$  are necessary to discuss the C phase. For instance,  $b_1$  and  $c_1$  determine the stability of the  $\sqrt{9} \times \sqrt{9}$  C phase [13] and the  $\sqrt{7} \times \sqrt{7}$  C phase (Supplemental Material Note 2 [23]),  $c_1$  determines the stability of the  $\sqrt{13} \times \sqrt{13}$  C phase [12], and so on. Moreover,  $e_i(\mathbf{Q}) = s\|\mathbf{Q} - \mathbf{Q}_{IC}^{(i)}\|^2/\|\mathbf{G}_i\|^2$ , where  $s$  is a constant, has been introduced to determine  $\mathbf{Q}_{IC}^{(i)}$ . [Other forms of  $e_i(\mathbf{Q})$  have also been proposed, which may be more appropriate in some experiments. See Supplemental Material Note 1 for consistency with other forms of  $e_i(\mathbf{Q}^{(i)})$  [23]]. Surprisingly, it was shown that the free energy Eq. (3) can also describe the NC phase in 1T-TaS<sub>2</sub> using the Nakanishi-Shiba expansion [12,13,24]

$$\psi_i(\mathbf{r}) = \sum_{\substack{l,m,n \geq 0 \\ l-m=n=0}} \Delta_{lmn}^{(i)} \exp\{i\mathbf{Q}_{lmn}^{(i)} \cdot \mathbf{r}\}, \quad (4)$$

where  $l, m, n$  are integers;  $\mathbf{Q}_{lmn}^{(i)} = \mathbf{Q}^{(i)} + l\mathbf{k}^{(i)} + m\mathbf{k}^{(i+1)} + n\mathbf{k}^{(i+2)}$ ,  $\mathbf{k}^{(i)} = \mu\mathbf{q}^{(i)} - \nu\mathbf{q}^{(i+1)}$  are CDW harmonics; and  $\mathbf{q}^{(i)} = \mathbf{Q}^{(i)} - \mathbf{Q}_C^{(i)}$  are domain-wall wave vectors. The free energy has been solved numerically by imposing a cutoff  $N \geq l, m, n \geq 0$ .  $N = 0$  represents the charge density modulation by the fundamental wave  $\mathbf{Q}^{(i)}$ . The free-energy

minimum for the NC phase appears as higher order harmonics  $N = 1, 2, 3, \dots$  are included.

Analytically, Eq. (3) can be integrated using Eq. (4) (see Supplemental Material Note 2 for a sample calculation, which is analogous to Refs. [12,13,23,24]). After integration, we obtain

$$F = \sum_{i=1}^3 \sum_{\substack{l,m,n \geq 0 \\ l \cdot m \cdot n = 0}} \Delta_{lmn}^{(i)*} \Delta_{lmn}^{(i)} e_i(\mathbf{Q}_{lmn}^{(i)}) + \dots, \quad (5)$$

where the terms in  $(\dots)$  are independent of  $\mathbf{Q}$ . The free energy is minimized by the condition

$$dF = \sum_{i=1}^3 \sum_{\substack{l,m,n \geq 0 \\ l \cdot m \cdot n = 0}} \frac{\partial F}{\partial \Delta_{lmn}^{(i)}} d\Delta_{lmn}^{(i)} + \sum_{i=1}^3 \nabla_{\mathbf{Q}^{(i)}} F \cdot d\mathbf{Q}^{(i)} = 0. \quad (6)$$

Regarding different  $\Delta_{lmn}^{(i)}$  and  $\mathbf{Q}^{(i)}$  as independent degrees of freedom and assuming that  $\Delta_{lmn}^{(i)}$  does not explicitly depend on  $\mathbf{Q}^{(i)}$ , then minimization of  $F$  requires us to solve the following differential equations:

$$\frac{\partial F}{\partial \Delta_{lmn}^{(i)}} = 0, \quad (7)$$

$$\nabla_{\mathbf{Q}^{(i)}} F = 0. \quad (8)$$

Equation (7), which contains all coefficients  $a(\mathbf{r}), b(\mathbf{r}), \dots, e_i(\mathbf{Q})$  in the free energy, leads to an infinite set of nonlinear differential equations which cannot be solved analytically. Numerical calculation of  $\Delta_{lmn}^{(i)}$  with fixed  $\mathbf{Q}^{(i)}$  has been done in our previous study [14], where we unveiled the existence of the multivalley free-energy landscape in  $1T$ -TaS<sub>2</sub> and  $2H$ -TaSe<sub>2</sub>. On the other hand, we show in the next section that Eq. (8) can be solved analytically, where the solution is a list of possible  $\mathbf{Q}$  vectors of DC-CDW phases.

*Conformal aspects of CDW phases.* In previous studies of CDW free energy, the free-energy local minima are obtained by calculating  $F$  for all values of  $\mathbf{Q}^{(i)}$ . However, we observe that local minima can also be obtained by differentiating  $F$  with respect to  $\mathbf{Q}^{(i)}$ . This major simplification is achieved by representing CDW vectors using complex numbers.

The correspondence  $(1, 0) \leftrightarrow 1$  and  $(0, 1) \leftrightarrow i = \sqrt{-1}$  maps  $\mathbf{a}_1$  and  $\mathbf{a}_2$  to  $a$  and  $a\omega$ , respectively, where  $\omega = e^{2\pi i/3} = -\frac{1}{2} + \frac{\sqrt{3}}{2}i$ . Then, the triangular lattice can be mapped to the set of *Eisenstein integers*  $\mathbb{Z}[\omega]$  with elements  $z = m + n\omega$  ( $m, n \in \mathbb{Z}$ ) [25]. Consequently,  $\mathbf{A}_C^{(i)}$  are equivalent to the Eisenstein integers [Fig. 1(a)]:

$$A_C = [(\mu + \nu) + \nu\omega]a, \quad A_C^{(i)} = A_C \omega^{i-1}. \quad (9)$$

$\mathbf{G}_i$  are mapped to  $G_i = 2\pi a^{-1} \omega^{1-i}$  and  $\mathbf{A}_C \cdot \mathbf{Q}_C = 2\pi$  corresponds to  $A_C^* Q_C = 2\pi$  where the asterisk denotes complex conjugation (this correspondence can be formalized, for instance, using 2D Clifford algebra [26]). Consequently,  $\mathbf{Q}_C^{(i)}$  are equivalent to

$$Q_C = \frac{2\pi}{A_C^*} = \frac{G_1}{\mu - \nu\omega}, \quad Q_C^{(i)} = Q_C \omega^{i-1}, \quad (10)$$

where we used Eqs. (9) and  $\omega^* = \omega^{-1} = \omega^2 = -1 - \omega$ . For brevity, we set  $G_1 = 1$  (i.e.,  $a = 2\pi$ ) in the following, which implies  $|G_i| = 1$  for  $i = 1, 2, 3$ .

We also write general CDW wave vectors  $\mathbf{Q}^{(i)} = (Q_x^{(i)}, Q_y^{(i)})$  using complex wave numbers  $Q^{(i)} = Q_x^{(i)} + iQ_y^{(i)}$ .  $\mathbf{q}^{(i)}$  and  $\mathbf{k}^{(i)}$  are also written using complex numbers (Fig. 1)

$$q^{(i)} = Q^{(i)} - Q_C^{(i)}, \quad k^{(i)} = \mu q^{(i)} - \nu q^{(i+1)}.$$

Using complex numbers the gradient  $\nabla_{\mathbf{Q}^{(i)}}$  is replaced by  $\partial/\partial Q^{(i)*}$ , so the CDW wave vectors for local minima between the C and IC phases are given as solutions of

$$\frac{\partial F}{\partial Q^{(i)*}} = \sum_{j=1}^3 \sum_{\substack{l,m,n \geq 0 \\ l \cdot m \cdot n = 0}} |\Delta_{lmn}^{(j)}|^2 \frac{\partial e_j(Q_{lmn}^{(j)})}{\partial Q^{(i)*}} = 0, \quad (11)$$

where

$$e_i(Q) = s(Q - Q_{IC}^{(i)})(Q^* - Q_{IC}^{(i)*}), \quad (12)$$

$$Q_{lmn}^{(i)} = Q^{(i)} + lk^{(i)} + mk^{(i+1)} + nk^{(i+2)}. \quad (13)$$

We solve Eq. (11) for three cases: (i) the isotropic NC phases, (ii) the T phases, and (iii) the stripe phases.

*a. The NC phases.* In the case of isotropic NC phases, we have the following simplification: (i) The wave vectors are separated by  $120^\circ$ , which implies  $Q^{(i+1)} = \omega Q^{(i)}$ . Consequently, (ii) the summation in Eq. (4) is a summation over Eisenstein integers  $z_{lmn} = l + m\omega + n\omega^2$  (note the identity  $\omega^2 + \omega + 1 = 0$ ) and (iii) the CDW harmonics have the simple expression  $k^{(i)} = \omega^{(i-1)}(Q/Q_C - 1)$ . Then, Eq. (13) with Eqs. (10) imply

$$Q_{lmn}^{(i)} = \frac{Q^{(i)}}{Q_C^{(1)}} (Q_C^{(1)} + z_{lmn}) - z_{lmn} \omega^{i-1}.$$

Using  $\partial Q/\partial Q^* = 0$ , we obtain

$$\begin{aligned} \frac{\partial F}{\partial Q^{(i)*}} &= s \sum_{j=1}^3 \sum_{\substack{l,m,n \geq 0 \\ l \cdot m \cdot n = 0}} |\Delta_{lmn}^{(j)}|^2 \\ &\times \left[ \frac{Q^{(j)}}{Q_C^{(1)}} (Q^{(1)} + z_{lmn}) - \omega^{j-1} (Q_{IC}^{(1)} + z_{lmn}) \right] \\ &\times \frac{\omega^{i-j}}{Q_C^{(1)*}} (Q_C^{(1)*} + z_{lmn}^*) \\ &= 0. \end{aligned} \quad (14)$$

We assume that components with different  $j$  values vanish individually such that the wave vector of the NC phase  $Q_{NC}^{(i)}$  is given by

$$\frac{Q_{NC}^{(i)}}{Q_C^{(i)}} = f(Q_{IC}^{(i)}) \equiv \frac{Q_{IC}^{(i)} + z_i}{Q_C^{(i)} + z_i}, \quad (15)$$

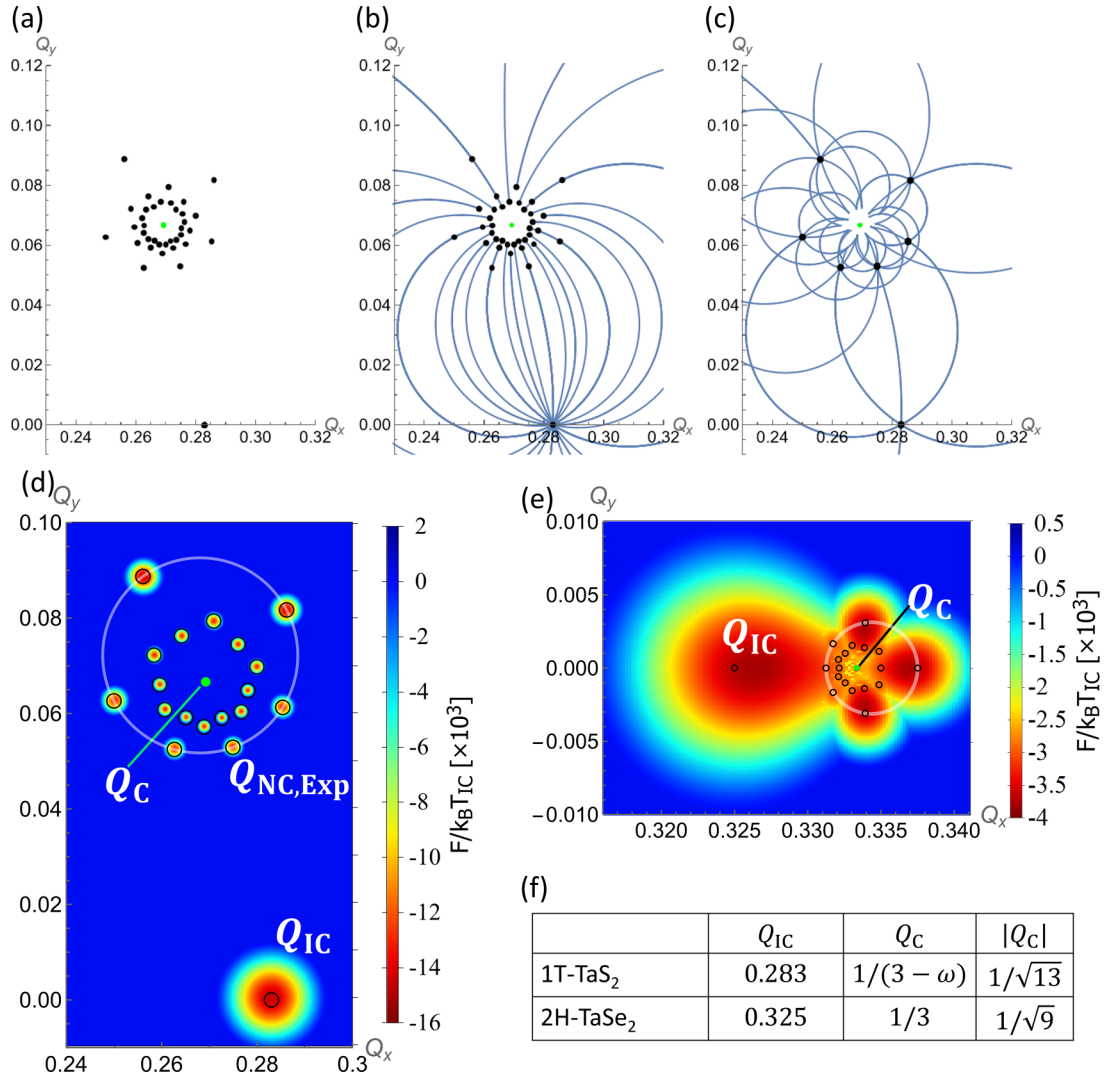


FIG. 2. (a) CDW local minima of 1T-TaS<sub>2</sub> are shown for  $N = 3$  harmonics in units with  $G_1 = 1$  (see also Supplemental Material Video 2 for larger  $N$  [23]). Different CDW free energy local minima correspond to distinct Eisenstein integers  $z_{lmn} = l + m\omega + n\omega^2$ . The green dot represents the C phase and the black dots [circles for (d) and (e)] represent local minima. (b) Each local minima is obtained from  $Q_{IC}$  by the action of Eq. (17). (c) Successive CDW phase transitions can be explained by a composition of Eq. (17). The local minima in the free-energy landscape for (d) 1T-TaS<sub>2</sub> and (e) 2H-TaSe<sub>2</sub> (obtained as in our previous work [14]) agrees with the local minima of Eq. (17). We used experimental values of wave vectors in (f).

where we defined the complex number

$$z_i = \frac{\sum_{l,m,n \geq 0} |\Delta_{lmn}^{(i)}|^2 \omega^{i-1} z_{lmn} (Q_C^{(1)*} + z_{lmn}^*)}{\sum_{l,m,n \geq 0} |\Delta_{lmn}^{(i)}|^2 (Q_C^{(1)*} + z_{lmn}^*)}. \quad (16)$$

Equation (15) shows that the wave vector of an NC phase can be obtained from the IC and C wave vectors with a complex number  $z_i$ . However, the form of  $z_i$  is complicated and gives little intuition, and we still need to solve for  $\Delta_{lmn}^{(i)}$  to obtain the numerical value of  $Q_{NC}^{(i)}$ . So, we investigate its meaning with the following approximation. In our previous work, we reported the free-energy landscape where different free-energy local minima correspond to distinct  $l, m, n$  values (Ref. [17]). Numerical results show that the amplitudes  $\Delta_{lmn}^{(i)}$  are localized near free energy local minima (Supplemental Material Fig. 3 [23]). Then, we have the approximation  $z_i \approx \omega^{i-1} z_{lmn}$ , which

implies that the wave vectors of NC phases corresponding to the free-energy local minima with the label  $lmn$  are given by the following solution:

$$\frac{Q_{NC,lmn}^{(1)}}{Q_C^{(1)}} = f_{lmn}(Q_{IC}^{(1)}) \equiv \frac{Q_{IC}^{(1)} + z_{lmn}}{Q_C^{(1)} + z_{lmn}}. \quad (17)$$

Equation (17) means that if  $Q_{IC}$  and  $Q_C$  are known, then CDW phases between IC and C are described by distinct Eisenstein integers  $z_{lmn}$  (Supplemental Material Video 1 [23]). Figure 2 shows the free energy local minima for  $\mu = 3$  and  $\nu = 1$  ( $\sqrt{13} \times \sqrt{13}$  C structure) with  $N = 3$  harmonics (see also Supplemental Material Video 2 for larger  $N$  [23]). We emphasize that the position of each local minima is determined from Eq. (8) which contains only the term

proportional to  $e_i$ . In other words, we find that the  $e_i$  term alone can explain the structure of the free energy landscape with a good approximation, without the need to solve for the amplitudes  $\Delta_{lmn}^{(i)}$ .

Mathematically, Eq. (15), which includes Eq. (17) as an approximation, is a conformal transformation. The set of transformations  $f$  have a one-to-one correspondence with a commutative subgroup of the projective linear group  $\text{PSL}(2, \mathbb{Z}[\omega])$ . This group property implies that transition between different local minima (different CDW phases) is obtained by a composition of  $f$  and  $f^{-1}$ . Three successive local minima lie on a circle whose center and radius can be calculated as in Supplemental Material Note 3 [23]: These can explain successive CDW phase transitions, such as the IC  $\rightarrow$  NC  $\rightarrow$  C phase transition in 1T-TaS<sub>2</sub> with decreasing temperature [14]. Figure 2(b) shows  $f_{lmn}(Q_{\text{IC}})$  for  $|z_{lmn}| \leq 3$ . This type of transformation can explain how each local minima is obtained from the IC phase. Figure 2(c) shows  $f_{lmn}(f_{l'm'n'}(Q_{\text{IC}}))$  for  $|z_{lmn}|, |z_{l'm'n'}| \leq 1$ . This transformation can explain successive CDW phase transitions. The free energy landscape in Fig. 2(d) 1T-TaS<sub>2</sub> and Fig. 2(e) 2H-TaSe<sub>2</sub> are obtained as in our previous work [14] (except for 2H-TaSe<sub>2</sub>, we used  $T - T_{\text{IC}} = -0.1$  to show local minima more clearly). We used experimental values of wave vectors

in Fig. 2(f). The free-energy calculation agrees with the local minima of Eq. (17).

*b. The T and stripe phases.* This conformal method also applies to anisotropic stripe and T phases as follows. Anisotropic CDW phases have domain walls that are tilted from each other by an angle that is different from 120°. This angle can be obtained with good accuracy using real-spacing imaging such as scanning tunneling microscope, so we use it as an input parameter.

Suppose that the domain wall wave vectors  $q^{(i)}$  of the T phase are related by  $q^{(1)} = w_1 q^{(1)}$ ,  $q^{(2)} = w_2 q^{(1)}$ , and  $q^{(3)} = w_3 q^{(1)}$ . For isotropic phases, we have  $w_2 = \omega$  and  $w_3 = \omega^2$ . Here,  $w_1 = 1$  is introduced for convenience such that the harmonic wave vectors are given by

$$k^{(i)} = (\mu w_i - \nu w_{i+1}) q^{(1)} \quad (18)$$

and  $Q_{lmn}^{(i)}$  can be written as

$$Q_{lmn}^{(i)} = \frac{Q^{(i)}}{Q_C^{(i)}} (Q_C^{(i)} + t_{i,lmn}) - t_{i,lmn}, \quad (19)$$

where we defined

$$t_{i,lmn} = \frac{(lw_i + mw_{i+1} + nw_{i+2})\mu - (lw_{i+1} + mw_{i+2} + nw_i)\nu}{w_i(\mu - \nu\omega)} \omega^{i-1}. \quad (20)$$

For isotropic phases, we obtain  $t_{i,lmn} = z_{lmn} \omega^{i-1}$  as expected. Consequently, Eq. (11) can be written as

$$\frac{\partial F}{\partial Q^{(i)*}} = s \sum_{j=1}^3 \sum_{\substack{l,m,n \geq 0 \\ l \cdot m \cdot n = 0}} |\Delta_{lmn}^{(j)}|^2 \left[ \frac{Q^{(j)}}{Q_C^{(j)}} (Q_C^{(j)} + t_{j,lmn}) - (Q_{\text{IC}}^{(j)} + t_{j,lmn}) \right] \frac{w_j^*}{w_i^*} \frac{1}{Q_C^{(j)*}} (Q_C^{(j)*} + t_{j,lmn}^*) = 0. \quad (21)$$

We assume that components with different  $j$  values vanish individually such that the wave vector of the T phase  $Q_{\text{T}}^{(i)}$  is given by

$$\frac{Q_{\text{T}}^{(i)}}{Q_C^{(i)}} = \frac{Q_{\text{IC}}^{(i)} + t_i}{Q_C^{(i)} + t_i}, \quad (22)$$

where we defined the complex number

$$t_i = \frac{\sum_{\substack{l,m,n \geq 0 \\ l \cdot m \cdot n = 0}} |\Delta_{lmn}^{(i)}|^2 t_{i,lmn} (Q_C^{(i)*} + t_{i,lmn}^*)}{\sum_{\substack{l,m,n \geq 0 \\ l \cdot m \cdot n = 0}} |\Delta_{lmn}^{(i)}|^2 (Q_C^{(i)*} + t_{i,lmn}^*)}. \quad (23)$$

If we further assume that different  $\Delta_{lmn}^{(i)}$  are localized near different local minima, then each local minima gives the T phase with the following wave vectors:

$$\frac{Q_{\text{T},lmn}^{(i)}}{Q_C^{(i)}} = \frac{Q_{\text{IC}}^{(i)} + t_{i,lmn}}{Q_C^{(i)} + t_{i,lmn}}. \quad (24)$$

Next, the stripe CDW phase has domain-wall wave vectors  $q^{(1)} = 0$  and  $q^{(2)} = -q^{(3)}$ . In this case, we have  $\Delta_{lmn}^{(1)} = 0$  so

$Q_{lmn}^{(2)}$  and  $Q_{lmn}^{(3)}$  can be written as

$$Q_{lmn}^{(2)} = \frac{Q^{(2)}}{Q_C^{(2)}} (Q_C^{(2)} + s_{2,lmn}) - s_{2,lmn},$$

$$Q_{lmn}^{(3)} = \frac{Q^{(3)}}{Q_C^{(3)}} (Q_C^{(3)} + s_{3,lmn}) - s_{3,lmn},$$

where we defined

$$s_{2,lmn} = \frac{(l-m)\mu - (n-l)\nu}{\mu - \nu\omega}, \quad (25)$$

$$s_{3,lmn} = \frac{(l-n)\mu - (n-m)\nu}{\mu - \nu\omega}, \quad (26)$$

which can also be obtained from Eq. (20) with  $w_1 \rightarrow 0$  and  $w_3 = -w_2$ . Consequently, Eq. (11) can be written as

( $i = 2, 3$ )

$$\begin{aligned} \frac{\partial F}{\partial Q^{(i)*}} = & -s \sum_{j=1,2} \sum_{\substack{l,m,n \geq 0 \\ l-m-n=0}} |\Delta_{lmn}^{(j)}|^2 \\ & \times \left[ \frac{Q_C^{(j)}}{Q_C^{(j)}} (Q_C^{(j)} + s_{j,lmn}) - (Q_{IC}^{(j)} + s_{j,lmn}) \right] \\ & \times \frac{1}{Q_C^{(j)*}} (Q_C^{(j)*} + s_{j,lmn}) = 0, \end{aligned} \quad (27)$$

where we have used  $\frac{\partial Q^{(2)}}{\partial Q^{(3)}} = -1$ . We assume that components with different  $j$  values vanish individually such that the wave vector of the stripe phase  $Q_S^{(i)}$  is given by

$$\frac{Q_S^{(i)}}{Q_C^{(i)}} = \frac{Q_{IC}^{(i)} + s_i}{Q_C^{(i)} + s_i}, \quad (28)$$

where we defined the complex number

$$s_i = \frac{\sum_{l,m,n \geq 0} |\Delta_{lmn}^{(i)}|^2 s_{i,lmn} (Q_C^{(i)*} + s_{i,lmn}^*)}{\sum_{l,m,n \geq 0} |\Delta_{lmn}^{(i)}|^2 (Q_C^{(i)*} + s_{i,lmn}^*)}. \quad (29)$$

If we further assume that different  $\Delta_{lmn}^{(i)}$  are localized near different local minima, then each local minima give the stripe phase with the following wave vectors:

$$\frac{Q_{S,lmn}^{(i)}}{Q_C^{(i)}} = \frac{Q_{IC}^{(i)} + s_{i,lm}}{Q_C^{(i)} + s_{i,lm}}. \quad (30)$$

It should be emphasized that the free energy local minima, which correspond to the NC, T, and stripe phases, are all obtained from Eq. (11). In the approximation where  $\Delta_{lmn}$  are localized near the local minima, a good approximation of the DC wave vectors was obtained from Eq. (8) only. This result is independent of the stability of each minima. Therefore, from this analysis, we reveal the different roles of stability and position in the CDW free-energy structure. From this point of view, isotropic and anisotropic DC-CDW phases can be clearly understood in a unified way.

*Consistency with experiments.* We have shown that the wave vectors of DC-CDW phases can be described by conformal transformations. Which of the local minima become stable depends on many factors such as temperature and sample thickness, but our method gives a list of possible  $Q$  vectors of new CDW phases. Since we have already shown the consistency with known CDWs, we test our theoretical results using experimental data. TaSe<sub>2</sub> thin films with thickness of 10 nm order have been synthesized by the dechalcogenide method. The details of this method are given in Refs. [8,27]. The CDW structure was observed by transmission electron microscope (TED). The crystal structure is shown in Figs. 3(a) and 3(b). Their TED patterns (obtained at room temperature) are shown in Figs. 3(d) and 3(e). Figure 3(d) is identified as the  $\sqrt{7} \times \sqrt{7}$  C phase as shown in Fig. 3(c) [8]. In addition to the C phase, a NC phase with  $|\mathbf{Q}_{NC}^{(1)}|/|\mathbf{G}_1| = 0.341(2)$  and  $\phi = 25.0(2)^\circ$  was observed in two different samples (Fig. 3(e) [27] and Supplemental Material Fig. 2) [23]. The fundamental NC wave vectors  $Q_{NC}^{(i)}$  are determined as in Supplemental Material Fig. 2 [23], where we made sure that the strongest satellite

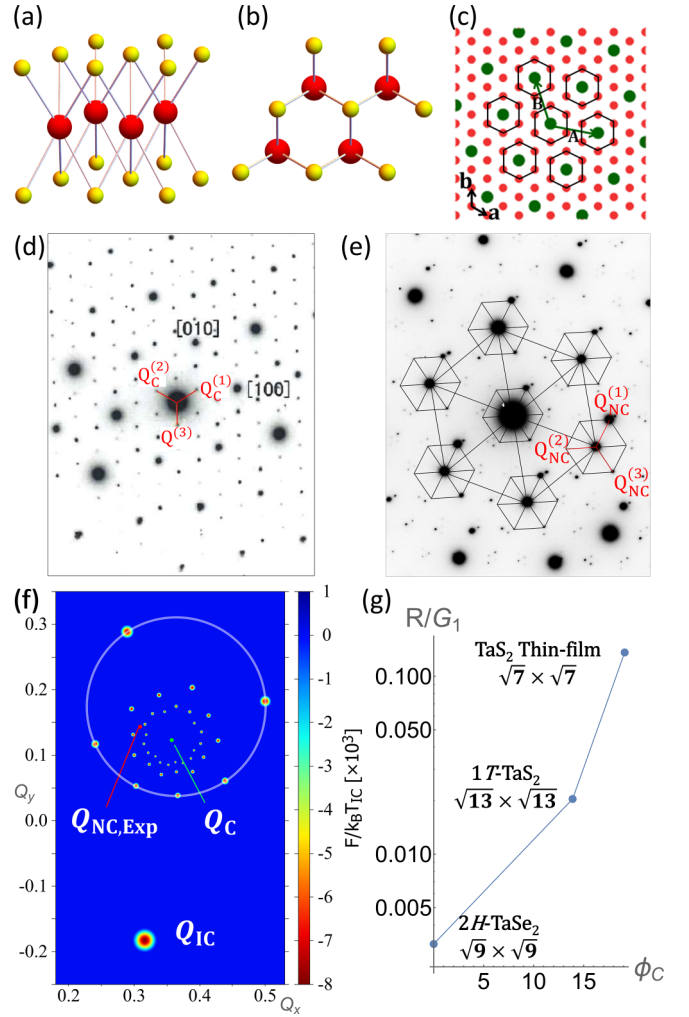


FIG. 3. (a) Structure of TaSe<sub>2</sub> thin film. Red spheres represent Ta atoms and yellow spheres represent Se atoms. (b) Top view of (a). (c) The  $\sqrt{7} \times \sqrt{7}$  commensurate structure involving seven atoms, a central Ta atom (green) surrounded by six Ta atoms (red), in the unit cell. TED pattern of (d)  $\sqrt{7} \times \sqrt{7}$  C phase [8] and (e) NC phase [27] in TaSe<sub>2</sub> thin film. (f) The CDW free energy landscape for TaSe<sub>2</sub> thin film is calculated as a function of a general wave vector  $\mathbf{Q} = (Q_x, Q_y)$  with  $N = 3$ . See Supplemental Material Note 5 [23] for free-energy parameters. The C phase is shown with a green dot. Experimental value of the NC phase is shown with a red dot. An enlarged image with local minima from Eq. (17) is shown in Supplemental Material Fig. 4 [23]. (g) Radius of circles shared by  $N = 1$  harmonics as a function of commensurate angle  $\phi_C$ .

peaks are included. Although it looks like the threefold rotational symmetry is broken, this is due to the inclination of the sample during the TEM measurement which affects the intensity of the CDW satellite peaks. To explain the appearance of this experimental NC phase, we first use Eq. (17) to see which local minimum it corresponds to, then we calculate the CDW free energy using Eq. (3).

The C and NC phases in TaSe<sub>2</sub> thin films are obtained at room temperature, so  $Q_{IC}$  with a much higher transition temperature could not be measured. However, we can obtain its approximate value based on the experimental NC phase. In 1T-TaS<sub>2</sub> and 2H-TaSe<sub>2</sub>,  $Q_C$  and  $Q_{IC}$  differ by no more than a

few percent [1,12,13]: We assume that this is also true for our TaSe<sub>2</sub> thin film.

Different  $MX_2$  polytypes can have different nesting mechanisms. The IC phase in  $2H$ -TaSe<sub>2</sub> can be formed by saddle point (van Hove singularity) nesting [19,20]. In thinner systems, the attractive force caused by the van Hove singularity could be stronger than the force caused by Fermi surface nesting. Saddle point nesting can occur both in the  $\Gamma$ - $M$  direction which is parallel to  $G_1$ , or in the  $\Gamma$ - $K$  ( $\Gamma$ - $K'$ ) which is tilted  $30^\circ$  ( $-30^\circ$ ) from  $G_1$ . From Ref. [19], one can estimate  $|Q_{IC}| = 0.53$  in the  $\Gamma$ - $M$  direction, but this value is too large. On the other hand, in the  $\Gamma$ - $K$  or  $\Gamma$ - $K'$  direction, one can estimate  $|Q_{IC}| = 0.31$  [19,20]. In fact, using Eq. (17), we observe that the local minimum  $f_{031}(Q_{IC})$  corresponds to the experimental NC phase if we set  $|Q_{IC}| = 0.35 \sim 0.38$  and  $\phi = -30^\circ$  (Supplemental Material Video 3 [23]). The  $-30^\circ$  angle implies that the IC phase in this sample is formed by van Hove singularity rather than Fermi-surface nesting.

In the above, we found that the experimental  $Q_{NC}$  value is included in the list of possible  $Q$ s if  $|Q_{IC}| = 0.35 \sim 0.38$  and  $\phi = -30^\circ$ . We confirm this result by calculating the free energy Eq. (3) numerically with the temperature dependence of the form  $a_0/2 = T - T_{IC}$  where  $T_{IC}$  is the IC-CDW transition temperature. The result of numerical calculation for TaSe<sub>2</sub> thin film is shown in Fig. 3. Note the multivalley free-energy landscape which coincides with the local minima obtained by the conformal method. If Eq. (17) was not available, one would need performing numerical calculations repeatedly by changing the values of  $Q_{IC}$  and other free-energy parameters. Even if a result is obtained that fits well with  $Q_{NC}$ , there is no guarantee whether this result is unique or whether it was obtained by chance. On the other hand, Eq. (17) allows us to determine the local minimum that fits  $Q_{NC}$  using only the values of  $Q_{IC}$  and  $Q_C$ . Then, if necessary, one can refine the free-energy parameters such that this minimum becomes stable. Therefore, we conclude that our method is ideal for analyzing CDW phases with almost no assumptions.

*Conclusion and discussion.* In this paper, we investigated the conformality of CDW in  $MX_2$  compounds. We showed that DC-CDW phases can be understood using conformal transformations. This method forms a basis to describe successive IC-DC-C phase transitions. If a CDW did not interact with the underlying base lattice, then  $Q^{(i)}$  may take arbitrary continuous values, so the discreteness of this transformation is due to the commensurability of CDW with the underlying base lattice. We also applied our analysis to experimental results of a NC phase in TaSe<sub>2</sub> thin-film with a  $\sqrt{7} \times \sqrt{7}$  C structure.

Why could we describe DC-CDW phases using a conformal transformation? Our reason is as follows. CDW has the aspect of a quantum crystal with a macroscopic wave function. The best way to describe a quantum crystal seems to be a method that keeps local angles and produces constant tension (crystal properties) and allows local deformations (wave property). It has been found that the deformation of 2D aperiodic lattices is governed by conformal transformations that satisfy these requirements [28,29]. Regarding CDWs as deformable superlattice crystals, it is reasonable that they can also be described by conformal transformations. Recall that

a conformal transformation refers to a composition of translation, rotation, dilation, and inversion [16]. The first three transformations can describe the change of CDW domain structure, and the last transformation connects the real-space structure to the momentum space. For nesting vectors that happen to be close to the C condition, there is a conformal law that locks in a CDW superlattice to the  $MX_2$  lattice. On the other hand, the ratio between the IC-CDW wave vector and the  $MX_2$  lattice constant is an irrational number, while that of the C-CDW wave vector is an integer. Therefore, a conformal description of CDW and the IC-DC-C CDW phase transitions should be described by a conformal function that connects continuous numbers (IC) and discrete numbers (C). So, a conformal method with complex numbers, which naturally satisfies these requirements, is ideal for studying CDW phases. In what follows, we give some implications of our results.

First, note that  $Q_C$  is a stationary point of the transformation (17), i.e.,  $f_{lmm}(Q_C) = 1$  (Supplemental Material Video 2 [23]). Therefore, we can regard  $Q_{IC}$  as a source,  $Q_C$  as a drain, and  $Q_{NC}$  as crossing points of the transformation. From this point of view, discommensuration may be understood as deviation from fixed points. This picture is a natural one because  $Q_{IC}$  values usually determine  $Q_C$ .

Second, in this paper, we described DC-CDW phases using the discrete conformal group  $PSL(2, \mathbb{Z}[\omega])$ , but a unified description of FQHL phases was also made using the discrete conformal group  $PSL(2, \mathbb{Z})$  [30–35]. These systems are both incompressible with a gapped spectrum. Therefore, we surmise that the field  $\mathbb{K}$  in the group  $PSL(2, \mathbb{K})$  is discrete for incompressible systems, and  $\mathbb{K}$  is continuous for compressible systems. These are summarized in Table I.

Third, local minima with the same value of  $|z_{lmm}|$  lie on a circle (Supplemental Material Note 2 [23]). Figures 2(d), 2(e) and 3(f) show the case with  $|z_{lmm}| = 1$ . Figure 3(g) shows the radius  $R$  of these circles as a function of the C angle  $\phi_C$ . Using experimental values of  $Q$  we find that  $R$  increases with  $\phi_C$ . The difference between  $|Q_C|$  and  $|Q_{IC}|$  in  $1T$ -TaS<sub>2</sub> ( $\sqrt{13} \times \sqrt{13}$  structure) and  $2H$ -TaSe<sub>2</sub> ( $\sqrt{9} \times \sqrt{9}$  structure) are both 2–3%, but the local minima are spread more widely (i.e., has larger  $R$ ) in  $1T$ -TaS<sub>2</sub>. On the other hand, NC is reported in  $1T$ -TaS<sub>2</sub> but not in  $2H$ -TaSe<sub>2</sub>. Moreover, our TaSe<sub>2</sub> thin film has large  $R$ , which allows  $|Q_C|$  and  $|Q_{IC}|$  to differ by more than 5%. Therefore, we surmise that, in addition to the norm of  $Q$ , the phase of  $Q$  must be considered to obtain a stable NC phase.

Fourth, we consider the temperature dependence of the IC-DC-C phase transition. The amplitudes  $\Delta_{lmm}$  change with temperature, which can be confirmed by calculating Eq. (7) numerically. So the wave vectors given by Eq. (15), Eq. (22), and Eq. (28) also change with temperature. If the amplitudes  $\Delta_{lmm}$  change smoothly with temperature, then  $Q$  will also change smoothly. The detail of transition depends on the choice of  $e_i(Q)$ . But, in any case, we confirm that the distribution of free-energy local minima barely changes (see Supplemental Material Fig. 1 [23]).

Fifth, we have shown that the variety of CDW domain structures can be understood using only the IC and C wave vectors. Therefore, our method is both simple and powerful, making it an ideal tool for analyzing CDW domain

TABLE I. Comparison of 2D electron systems and their representative groups. The incompressibility of a system is associated with the presence of a band gap. We surmise that field  $\mathbb{K}$  in group  $\text{PSL}(2, \mathbb{K})$  is discrete for incompressible systems, and  $\mathbb{K}$  is continuous for compressible systems.

2D system	Compressibility/gap type	Material	Group
$\text{IC}_1 \leftrightarrow \text{IC}_2$	Compressible? [21]	$\text{MX}_2$	$\text{PSL}(2, \mathbb{C})$
$\text{IC} \leftrightarrow \text{NC}$		1T-TaS <sub>2</sub>	
$\text{NC}_1 \leftrightarrow \text{NC}_2$	Incompressible, [31] Comme. gap	TaSe <sub>2</sub> thin-film	$\text{PSL}(2, \mathbb{Z}[\omega])$
$\text{IC} \leftrightarrow \text{C}$		2H-TaSe <sub>2</sub> VSe <sub>2</sub>	
QHL	Incompressible, magnetoroton gap	GaAs	$\text{PSL}(2, \mathbb{Z})$

walls. For example, we can show that the DC structure in Cu-doped TiSe<sub>2</sub> (with  $\sqrt{4} \times \sqrt{4}$  C structure) [36] can be understood as the T phase and stripe phase. On the other hand, the McMillan-Nakanishi-Shiba model can give only free-energy results that are averaged over the system. Therefore, some of the results reported in Ref. [36], such as the disappearance of domain wall by removal of impurity, are not covered by our results. On the other hand, our theory can predict what kind of domain-wall structure (wave vectors) can appear.

Finally, possible future studies are as follows. Our conformal method, which keeps angles and produces constant tension (crystal properties) and allows local deformations

(wave property), is ideal for describing CDWs as quantum crystals and would be applicable to quantum liquid crystals and Moiré solids. We expect that our formalism is also applicable to other superlattice systems [37,38]: <sup>3</sup>He A/B interface [39] and other triple-Q systems like skyrmion lattices. Although we have focused on a triangular lattice, similar results may be obtained in square lattice *mutatis-mutandis* using Gauss integers  $\mathbb{Z}[i]$  with elements  $z = a + ib$ ,  $a, b \in \mathbb{Z}$  to describe CDWs in CuO, FeTe, and charge order.

*Acknowledgments.* The authors thank the Supercomputer Center, the Institute for Solid State Physics, and the University of Tokyo for use of the facilities. T.N.I. was supported by JSPS KAKENHI Grants No. JP18K13495 and No. 21K13852.

- 
- [1] J. Wilson, F. J. Di Salvo, and S. Mahajan, *Adv. Phys.* **24**, 117 (1975).  
[2] G. Grüner, *Rev. Mod. Phys.* **60**, 1129 (1988).  
[3] P. Monceau, *Adv. Phys.* **61**, 325 (2012).  
[4] R. M. Fleming, D. E. Moncton, D. B. McWhan, and F. J. Di Salvo, *Phys. Rev. Lett.* **45**, 576 (1980).  
[5] S. Tanda, T. Sambongi, T. Tani, and S. Tanaka, *J. Phys. Soc. Jpn.* **53**, 476 (1984).  
[6] S. Tanda and T. Sambongi, *Synth. Met.* **11**, 85 (1985).  
[7] M. Yoshida, R. Suzuki, Y. Zhang, M. Nakano, and Y. Iwasa, *Sci. Adv.* **1**, e1500606 (2015).  
[8] T. Toshima, K. Inagaki, N. Hatakenaka, and S. Tanda, *J. Phys. Soc. Jpn.* **75**, 024706 (2006).  
[9] L. Stojchevska, I. Vaskivskiy, T. Mertelj, P. Kusar, D. Svetin, S. Brazovskii, and D. Mihailovic, *Science* **344**, 177 (2014).  
[10] W. L. McMillan, *Phys. Rev. B* **14**, 1496 (1976).  
[11] K. Inagak (private communication); K. Inagaki and S. Tanda, *Phys. Rev. B* **97**, 115432 (2018).  
[12] K. Nakanishi and H. Shiba, *J. Phys. Soc. Jpn.* **43**, 1839 (1977).  
[13] K. Nakanishi and H. Shiba, *J. Phys. Soc. Jpn.* **44**, 1465 (1978).  
[14] K. Nakatsugawa, S. Tanda, and T. N. Ikeda, *Sci. Rep.* **10**, 1239 (2020).  
[15] D. Sakabe, Z. Liu, K. Suenaga, K. Nakatsugawa, and S. Tanda, *npj Quantum Mater.* **2**, 22 (2017).  
[16] G. A. Jones and D. Singerman, *Complex Functions: An Algebraic and Geometric Viewpoint* (Cambridge University Press, Cambridge, 1987).  
[17] P. B. Littlewood and T. M. Rice, *Phys. Rev. Lett.* **48**, 27 (1982).  
[18] L. Van Hove, *Phys. Rev.* **89**, 1189 (1953).  
[19] T. M. Rice and G. K. Scott, *Phys. Rev. Lett.* **35**, 120 (1975).  
[20] A. H. Castro Neto, *Phys. Rev. Lett.* **86**, 4382 (2001).  
[21] S.-J. Yang, Y. Yu, and Z.-B. Su, *Phys. Rev. B* **62**, 13557 (2000).  
[22] Y. Yamada and H. Takatera, *Solid State Commun.* **21**, 41 (1977).  
[23] See Supplemental Material at <http://link.aps.org/supplemental/10.1103/PhysRevB.109.L081407> for consistency with previous studies, derivation of free energy, detail of conformal structure, additional figures and supplemental videos.  
[24] K. Nakanishi, H. Takatera, Y. Yamada, and H. Shiba, *J. Phys. Soc. Jpn.* **43**, 1509 (1977).  
[25] J. Conway, *The Book of Numbers* (Copernicus, New York, NY, 1996).  
[26] D. Hestenes and G. Sobczyk, *Clifford Algebra to Geometric Calculus: A Unified Language for Mathematics and Physics* (D. Reidel, Dordrecht, 1987).  
[27] T. Toshima, Ph.D. thesis, Department of Applied Physics, Hokkaido University, 2006.  
[28] F. Rothen, P. Pierański, N. Rivier, and A. Joyet, *Eur. J. Phys.* **14**, 227 (1993).  
[29] F. Rothen and P. Pierański, *Phys. Rev. E* **53**, 2828 (1996).  
[30] A. Belavin, A. Polyakov, and A. Zamolodchikov, *Nucl. Phys. B* **241**, 333 (1984).  
[31] R. B. Laughlin, *Phys. Rev. Lett.* **50**, 1395 (1983).  
[32] C. A. Lütken and G. G. Ross, *Phys. Rev. B* **45**, 11837 (1992).  
[33] S. Kivelson, D.-H. Lee, and S.-C. Zhang, *Phys. Rev. B* **46**, 2223 (1992).  
[34] K. S. Olsen, H. S. Limseth, and C. A. Lütken, *Phys. Rev. B* **97**, 045113 (2018).

- [35] T. H. Hansson, M. Hermanns, S. H. Simon, and S. F. Viefers, [Rev. Mod. Phys.](#) **89**, 025005 (2017).
- [36] S. Yan, D. Iaia, E. Morosan, E. Fradkin, P. Abbamonte, and V. Madhavan, [Phys. Rev. Lett.](#) **118**, 106405 (2017).
- [37] P. Bak, [Rep. Prog. Phys.](#) **45**, 587 (1982).
- [38] Y. Bai, T. Jian, Z. Pan, J. Deng, X. Lin, C. Zhu, D. Huo, Z. Cheng, Y. Liu, P. Cui, Z. Zhang, Q. Zou, and C. Zhang, [Nano Lett.](#) **23**, 2107 (2023).
- [39] G. E. Volovik, *The Universe in a Helium Droplet* (Oxford University Press, New York, 2009).